Role of the Vortex-Core Energy on the Berezinskii-Kosterlitz-Thouless Transition in Thin Films of NbN

Mintu Mondal,[1] Sanjeev Kumar,[1] Madhavi Chand,[1] Anand Kamlapure,[1] Garima Saraswat,[1]
G. Seibold,[2] L. Benfatto,[3,*] and Pratap Raychaudhuri[1,†]

[1]*Tata Institute of Fundamental Research, Homi Bhabha Road, Colaba, Mumbai, 400005, India*
[2]*Institut Für Physik, BTU Cottbus, P.O. Box 101344, 03013 Cottbus, Germany*
[3]*ISC-CNR and Department of Physics, Sapienza University of Rome, Piazzale Aldo Moro 5, 00185, Rome, Italy*
(Received 10 August 2011; published 14 November 2011)

We analyze the occurrence of the Berezinskii-Kosterlitz-Thouless (BKT) transition in thin films of NbN at various film thickness, by probing the effect of vortex fluctuations on the temperature dependence of the superfluid density below T_{BKT} and of the resistivity above T_{BKT}. By direct comparison between the experimental data and the theory, we show the crucial role played by the vortex-core energy in determining the characteristic signatures of the BKT physics, and we estimate its dependence on the disorder level. Our work provides a paradigmatic example of BKT physics in a quasi-two-dimensional superconductor.

DOI: 10.1103/PhysRevLett.107.217003 PACS numbers: 74.40.−n, 74.62.En, 74.70.Ad, 74.78.−w

Ever since the pioneering work of Berezinskii, Kosterlitz, and Thouless (BKT) [1,2] predicting the occurrence of a phase transition without a continuously broken symmetry in quasi-two-dimensional (2D) systems, a lot of effort has been devoted to study its realization in real materials [3]. Of particular interest have been 2D superconductors [4–11], where the superconducting (SC) transition is expected to belong to the BKT universality class. In these systems, the BKT transition can be studied through two different schemes. When approaching the transition temperature T_{BKT} from below, the superfluid density n_s (which is related to the magnetic penetration depth λ) is expected to go to zero discontinuously at the transition, with a "universal" relation between $n_s(T_{\mathrm{BKT}})$ and T_{BKT} itself [3,12]. Approaching the transition from above, one can identify the BKT transition from SC fluctuations, which leave their signature in the temperature dependence of various quantities, such as resistivity or magnetization [13]. In this second scheme, the information on the BKT transition is encoded in the correlation length $\xi(T)$, which diverges exponentially at T_{BKT}, in contrast to the power-law dependence expected within Ginzburg-Landau (GL) theory [14].

Many of the experimental investigations on 2D superconductors have relied on this second approach [7–10] to identify the BKT transition through the temperature dependence of resistivity $\rho(T)$, using eventually the interpolating formula proposed long ago by Halperin and Nelson [13] to describe the crossover from BKT to ordinary GL superconducting fluctuations. However, real superconductors have additional complicacies that can make such an analysis more involved than what has been discussed in the original theoretical approach. First, real systems always have some degree of inhomogeneity, which tends to smear the sharp signatures of BKT transition compared to the clean case. As it has been recently shown through scanning tunneling spectroscopy measurements [15,16], even when disorder in the system is homogeneous, the system shows an intrinsic tendency towards the formation of spatial inhomogeneity in the SC state, which has to be taken into account while analyzing the BKT transition. At a more fundamental level, it has recently been proved experimentally [6] that, for a real superconductor, the vortex-core energy μ can be very different from the value predicted within the 2D XY model, which was originally investigated by Kosterlitz and Thouless as the paradigmatic case to study the BKT transition [2]. This can give rise to a somehow different manifestation of the vortex physics, even without the extreme of a change of the order of the transition, as it has been proposed in the past [3,17]. Recently, the relevance of μ for the BKT transition has attracted a renewed theoretical interest in different contexts, ranging from the case of layered high-temperature superconductors [18–20] to the one of superconducting interfaces in artificial heterostructures [21].

All the above issues explain why, more than 30 years after the prediction of the BKT transition in ultrathin films of superconductors, its occurrence in real materials is still controversial. The present Letter aims to give a paradigmatic example of the emergence of the BKT transition in thin films of NbN as the film thickness decreases. By a systematic comparison between $\lambda(T)$ and $\rho(T)$, we show that, to fully capture the "conventional" BKT behavior in a real system, one must account for the correct value of μ as compared to the energy scale given by the superfluid stiffness J_s. The analysis carried out for films of different thickness provides us also with an indirect measurement of the dependence of the vortex-core energy on disorder, showing that vortices become energetically more expensive as disorder increases. Such a result can be related to the separation between the energy scales connected to the SC gap, Δ, and J_s as disorder increases, as we show by computing the ratio μ/J_s within the Bogoliubov–de Gennes solution of the attractive Hubbard model with on-site disorder. Our results shed new light on the occurrence of the BKT transition on disordered films.

Our samples consist of epitaxial NbN films grown on single-crystalline (100) oriented MgO substrates with thickness d varying between 3–50 nm. The deposition conditions were optimized to obtain the highest T_c (16 K) for a 50 nm thick film. Details of sample preparation and characterization have been reported elsewhere [6,22]. The absolute value of λ as a function of temperature was measured using a low-frequency (60 kHz) two-coil mutual inductance technique [6] on 8 mm diameter films patterned using a shadow mask. $\rho(T)$ was measured on the same films through conventional four-probe technique after pattering the films into 1 mm $\times$ 6 mm striplines using Ar-ion milling.

The first clear signature of the presence of vortices in our samples is provided by the deviations of $\lambda^{-2}(T)$ from the BCS temperature dependence as d decreases. In particular, we observe a sharp downturn of $\lambda^{-2}(T)$, reminiscent of the so-called universal jump of the superfluid density [12]. To clarify the notation, we recall that, for a 2D superconductor, J_s is defined as

$$J_s = \frac{\hbar^2 n_s^{2d}}{4m} = \frac{\hbar^2 c^2 d}{16\pi e^2 \lambda^2}, \tag{1}$$

where n_s^{2d} is the effective 2D superfluid density. In a conventional 3D superconductor, $J_s(T)$ goes to zero continuously at the SC temperature T_c. Instead, within BKT theory, the SC transition is controlled by the vortex-antivortex proliferation that becomes entropically favorable at the temperature scale $T_{\rm BKT}$ defined self-consistently by the relation

$$\frac{\pi J_s(T_{\rm BKT})}{T_{\rm BKT}} = 2. \tag{2}$$

In the above relation, the temperature dependence of $J_s(T)$ is due not only to the existence of quasiparticle excitations above the gap but also to the presence of bound vortex-antivortex pairs *below* $T_{\rm BKT}$. The latter effect is usually negligible when μ is large, as is the case for superfluid films [23]. In this case, one can safely estimate $T_{\rm BKT}$ as the temperature where the line $2T/\pi$ intersects the $J_s^{\rm BCS}(T)$ obtained by a BCS fit of the superfluid stiffness at lower temperatures. However, as μ decreases, the renormalization of J_s due to bound vortex pairs increases, and consequently $T_{\rm BKT}$ is further reduced with respect to T_c [6,18]. To account for this effect, we fitted the temperature dependence of $\lambda^{-2}(T)$ by integrating numerically the renormalization-group (RG) equations of the BKT theory [3,18] using the ratio μ/J_s as the only free parameter [6]. As an input parameter for $J_s(T)$, we used the one obtained by a BCS fit of the data [solid lines in Fig. 1(a)] at low temperatures, where vortex excitations are suppressed, which extrapolates to zero at the mean-field transition temperature T_c. As one can see in Fig. 1(b), the transition is still slightly rounded near $T_{\rm BKT}$, so that the sharp jump is replaced by a rapid downturn at the intersection with the universal $2T/\pi$ line. We attribute this effect to the spatial inhomogeneity of the sample, which can be accounted for by assuming a distribution of local $J_s^i(T)$ values around the BCS one, and performing an average of the $\lambda^{-2}(T)$ associated to each patch [24]. For simplicity, we assume that the occurrence probability w_i of each local J_s^i value is Gaussian, with relative width δ. We then rescale proportionally the local T_c^i and calculate the resulting $T_{\rm BKT}^i$ from the RG equations [6,19]. As shown in Figs. 1(a) and 1(b), such a procedure leads to an excellent fit of the experimental data in the whole temperature range. The obtained values of the ratio μ/J_s (Table I) are relatively small as compared to the standard expectation of the XY model [25], where

$$\frac{\mu_{XY}}{J_s} \simeq \frac{\pi^2}{2} \simeq 4.9. \tag{3}$$

We recall that, within the BKT approach to the XY model, the value of μ is fixed by the cutoff at short length scales of the energy of a vortex line,

$$E = \pi J_s\left[\log\frac{L}{\xi_0} + \alpha\right], \tag{4}$$

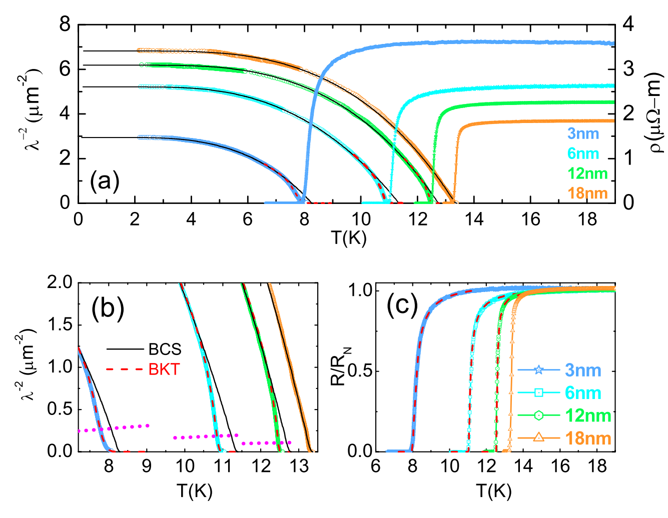

FIG. 1 (color online). (a) Temperature dependence of $\lambda^{-2}(T)$ and $\rho(T)$ for four NbN films with different thickness. The solid (black) lines and dashed (red) lines correspond to the BCS and BKT fits of the $\lambda^{-2}(T)$ data, respectively. (b) An expanded view of $\lambda^{-2}(T)$ close to $T_{\rm BKT}$; the intersection of the BCS curve with the dotted line is where the BKT jump would be expected within the XY model, when μ is large. (c) Temperature variation of R/R_N. The dashed (red) lines show the theoretical fits to the data, as described in the text.

where L is the system size, ξ_0 is the coherence length, and $\mu \equiv \pi J_s \alpha$. By mapping the (lattice) XY model into the continuum Coulomb-gas problem [25], one obtains $\alpha \simeq \pi/2$, so that μ attains the value in Eq. (3). However, in our samples, μ is better estimated from the loss of condensation energy within the vortex core (see discussion below), leading to a smaller μ/J_s ratio and to the deviations of the data from the BCS fit already before the renormalized stiffness reaches the universal value $2T/\pi$.

To further establish the validity of the values of μ obtained from the behavior of $\lambda^{-2}(T)$ *below* $T_{\rm BKT}$, we now use the same set of parameters to analyze the $\rho(T)$ *above* $T_{\rm BKT}$. In 2D, the contribution of SC fluctuations to the conductivity can be encoded in the temperature dependence of the SC correlation length, $\delta\sigma \propto \xi^2(T)$. The functional form of $\xi(T)$ depends on the character of the SC fluctuations, being power-law for Gaussian GL fluctuations [14] and exponential for BKT-like vortex fluctuations [2,13]. Because of the proximity between $T_{\rm BKT}$ and T_c (Table I), we expect that most of the fluctuation regime for the paraconductivity will be described by standard GL SC fluctuations, while vortex fluctuations will be relevant only between T_c and $T_{\rm BKT}$. To interpolate between the two regimes, we resort then to the Halperin-Nelson formula for ξ [13],

$$\frac{\xi}{\xi_0} = \frac{2}{A} \sinh\frac{b}{\sqrt{t}}, \tag{5}$$

where $t = (T - T_{\rm BKT})/T_{\rm BKT}$ and A is a constant of order one. b is the most relevant parameter to determine the shape of the resistivity above the transition and is connected [21] both to the relative distance t_c between $T_{\rm BKT}$ and T_c, $t_c = (T_c - T_{\rm BKT})/T_{\rm BKT}$, and to the value of μ:

$$b_{\rm theo} \sim \frac{4}{\pi^2}\frac{\mu}{J_s}\sqrt{t_c}. \tag{6}$$

The normalized resistance corresponding to the SC correlation length (5) is given by

$$\frac{R}{R_N} = \frac{1}{1 + (\Delta\sigma/\sigma_N)} \equiv \frac{1}{1 + (\xi/\xi_0)^2}, \tag{7}$$

where R_N is the normal-state resistance [that we take here as $R_N \equiv R(T = 1.5T_{\rm BKT})$]. Finally, to account for sample inhomogeneity, we map the spatial inhomogeneity of the sample in a random-resistor-network problem, by associating to each patch of stiffness J_s^i a normalized resistance $\rho_i = R_i/R_N$ obtained from Eq. (7) by using the corresponding local values of T_c^i and $T_{\rm BKT}^i$ computed above. The overall sample normalized resistance $\rho = R/R_N$ is then calculated in the so-called effective-medium-theory approximation [26], where ρ is the solution of the self-consistent equation

$$\sum_i \frac{w_i(\rho - \rho_i)}{\rho + \rho_i} = 0 \tag{8}$$

and w_i is the occurrence probability of each resistor, i.e., of the corresponding J_s^i value, as determined by the analysis below $T_{\rm BKT}$. As it has been discussed in Ref. [27], the effective-medium-theory approach turns out to be in excellent agreement with the exact numerical results for a network of resistors undergoing a metal-superconductor transition, even in the presence of SC fluctuations. We can then employ Eq. (8) to compute R/R_N of our samples, by using the probability distribution of width δ known from the analysis of $\lambda(T)$ and by treating A and b as free parameters. The resulting fits are in excellent agreement with the experimental data [Fig. 1(c)]. Moreover, considering that the interpolation formula (5) between the BKT and GL fluctuation regime is necessarily an approximation, the obtained values of b are in very good agreement with the theoretical estimate (6) (Table I). Thus, our analysis above T_c not only provides us with a remarkable example of interpolation between the GL and BKT fluctuation regimes but it also demonstrates the validity of the values of μ obtained from $\lambda(T)$. Finally, we would like to stress that b cannot be used completely as a free parameter while fitting the $\rho(T)$. Attempting to fit the BKT fluctuation regime at $T \gg T_{\rm BKT}$ (as proposed in the literature [8,9]) results in unphysical b values with respect to relation (6).

Once the robustness of our estimate of μ is established, we discuss now the values reported in Table I and their thickness dependence. We first notice that the values of μ

TABLE I. Sheet resistance (R_s), magnetic penetration depth [$\lambda(T \to 0)$], $T_{\rm BKT}$, and BCS transition temperature T_c, along with the best fit parameters (see text) obtained from the BKT fits of $\lambda^{-2}(T)$ below $T_{\rm BKT}$ and of $R(T)$ above $T_{\rm BKT}$ for NbN thin films of different thicknesses d. The temperature T_c is obtained by the extrapolation of the BCS fit of λ^{-2} well below $T_{\rm BKT}$.

					Fit of $\lambda^{-2}(T)$			Fit of $R(T)$	
d (nm)	R_s ($k\Omega$)	$\lambda(0)$ (nm)	$T_{\rm BKT}$ (K)	T_c (K)	μ/J_s	δ/J_s	$b_{\rm theo}$	A	b
3	1.2	582	7.77	8.3	1.19	0.02	0.108	1.35	0.108
6	0.44	438	10.85	11.4	0.61	0.005	0.048	1.3	0.067
12	0.19	403	12.46	12.8	0.46	0.0015	0.027	1.21	0.039
18	0.1	383	···	13.37	···	···	···	···	···

obtained by our fit are of the order of magnitude of the standard expectation for a BCS superconductor. Indeed, in this case, one usually [28] estimates the μ as the loss in condensation energy within a vortex core of the size of the order of the coherence length ξ_0,

$$\mu = \pi \xi_0^2 \epsilon_{\mathrm{cond}}, \tag{9}$$

where ϵ_{cond} is the condensation-energy density. In the clean case, Eq. (9) can be expressed in terms of J_s by means of the BCS relations for ϵ_{cond} and ξ_0. Indeed, since $\epsilon_{\mathrm{cond}} = N(0)\Delta^2/2$, where $N(0)$ is the density of states at the Fermi level and Δ is the BCS gap; $\xi_0 = \xi_{\mathrm{BCS}} = \hbar v_F/\pi\Delta$, where v_F is the Fermi velocity; and assuming that $n_s = n$ at $T = 0$, where $n = 2N(0)v_F^2 m/3$, one has

$$\mu_{\mathrm{BCS}} = \frac{\pi \hbar^2 n_s}{4m} \frac{3}{\pi^2} = \pi J_s \frac{3}{\pi^2} \simeq 0.95 J_s, \tag{10}$$

so that it is quite smaller than in the XY-model case (3). While the exact determination of μ depends on small numerical factors that can slightly affect the above estimate, the main ingredient that we should still account for is the effect of disorder that can alter the relation between ϵ_{cond}, Δ, and J_s and explain the variations observed experimentally. To properly account for it, we computed explicitly both μ and J_s within the attractive two-dimensional Hubbard model with local disorder:

$$H = -t \sum_{\langle ij \rangle \sigma} (c_{i\sigma}^\dagger c_{j\sigma} + \mathrm{H.c.}) - |U| \sum_i n_{i\uparrow} n_{i\downarrow} + \sum_{i\sigma} V_i n_{i\sigma}, \tag{11}$$

which we solve in the mean field using the Bogoliubov–de Gennes equations [29]. The first sum is over nearest-neighbor pairs, and we work on a $N = N_x \times N_y$ system, with a local potential V_i randomly distributed between $0 \le V_i \le V_0$. J_s is computed by the change in the ground-state energy in the presence of a constant vector potential [30], while μ is computed by means of Eq. (9), by determining both ϵ_{cond} and ξ in the presence of disorder [31] at doping $n = 0.87$ and coupling $U/t = 1$. The resulting value of μ/J_s at $T = 0$ is reported in Fig. 2(a): It is of the order of the BCS estimate and it shows a steady increase as disorder increases, in agreement with the experimental results, shown in Fig. 2(b), where we take the normal-state sheet resistance R_s as a measure of disorder as the film thickness decreases. This behavior can be understood as a consequence of the increasing separation with disorder between the energy scales associated, respectively, to the Δ, which controls ϵ_{cond}, and J_s, as it is shown by the ratio Δ/J_s that we report in the two panels of Fig. 2 for comparison. Notice that, even though we used a weaker coupling $U/t = 1$ as compared to other recent studies [30,32], this is still a large coupling strength as compared to our NbN samples, so that the numerical values of Δ/J_s are larger than experimental ones [33]. Nonetheless, our approach already captures the experimental trend of μ/J_s as a function of disorder and its correlation with the Δ/J_s behavior at large disorder.

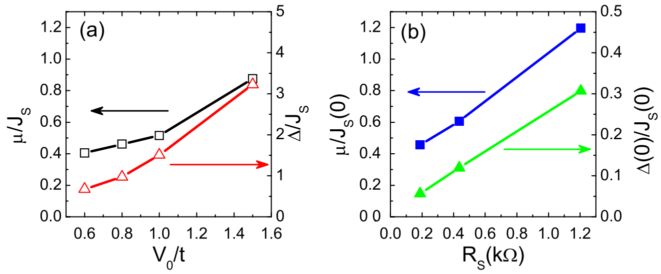

FIG. 2 (color online). (a) Numerical results for the disorder dependence of μ/J_s and Δ/J_s as a function of disorder for the attractive Hubbard model. (b) Experimental values for the same ratios in our NbN films, plotted as a function of the normal-state sheet resistance R_s.

In summary, we have shown that, to correctly identify the typical signatures of the BKT transition in thin films of NbN, we must properly account for μ values smaller than expected within the standard approach based on the XY model [1,2]. We also observe steady increases of the ratio μ/J_s as the film thickness decreases. This effect can be understood within a model for disordered superconductors, resulting from increasing separation between the energy scales associated with Δ and J_s. It would be interesting to investigate if a similar effect could be at play also in other systems, as disordered films of InO_x [5] or high-temperature cuprate superconductors, where a large μ value has been indirectly suggested by the analysis of the superfluid density data [18].

We acknowledge Vivas Bagwe and John Jesudasan for technical support.

*Lara.Benfatto@roma1.infn.it
†pratap@tifr.res.in

[1] V. L. Berezinskii, Sov. Phys. JETP **34**, 610 (1972); J. M. Kosterlitz and D. J. Thouless, J. Phys. C **6**, 1181 (1973).
[2] J. M. Kosterlitz, J. Phys. C **7**, 1046 (1974).
[3] P. Minnhagen, Rev. Mod. Phys. **59**, 1001 (1987).
[4] A. T. Fiory, A. F. Hebard, and W. I. Glaberson, Phys. Rev. B **28**, 5075 (1983).
[5] W. Liu, M. Kim, G. Sambandamurthy, and N. P. Armitage, Phys. Rev. B **84**, 024511 (2011).
[6] A. Kamlapure, M. Mondal, M. Chand, A. Mishra, J. Jesudasan, V. Bagwe, L. Benfatto, V. Tripathi, and P. Raychaudhuri, Appl. Phys. Lett. **96**, 072509 (2010).
[7] N. Reyren, S. Thiel, A. D. Caviglia, L. Fitting Kourkoutis, G. Hammerl, C. Richter, C. W. Schneider, T. Kopp, A.-S. Ruetschi, D. Jaccard, M. Gabay, D. A. Muller, J.-M. Triscone, and J. Mannhart, Science **317**, 1196 (2007).
[8] A. D. Caviglia, S. Gariglio, N. Reyren, D. Jaccard, T. Schneide, M. Gabay, S. Thiel, G. Hammerl, J. Mannhart, and J.-M. Triscone, Nature (London) **456**, 624 (2008).

[9] J. T. Ye, S. Inoue, K. Kobayashi, Y. Kasahara, H. T. Yuan, H. Shimotani, and Y. Iwasa, Nature Mater. **9**, 125 (2010).

[10] D. Matthey, N. Reyren, J.-M. Triscone, and T. Schneider, Phys. Rev. Lett. **98**, 057002 (2007).

[11] P. K. Rout and R. C. Budhani, Phys. Rev. B **82**, 024518 (2010).

[12] D. R. Nelson and J. M. Kosterlitz, Phys. Rev. Lett. **39**, 1201 (1977).

[13] B. I. Halperin and D. R. Nelson, J. Low Temp. Phys. **36**, 599 (1979).

[14] A. Larkin and A. A. Varlamov, *Theory of Fluctuations in Superconductors* (Oxford University Press, New York, 2009), 2nd ed.

[15] B. Sacépé, C. Chapelier, T. I. Baturina, V. M. Vinokur, M. R. Baklanov, and M. Sanquer, Nature Commun. **1**, 140 (2010); B. Sacépé, T. Dubouchet, C. Chapelier, M. Sanquer, M. Ovadia, D. Shahar, M. Feigel'man, and L. Ioffe, Nature Phys. **7**, 239 (2011).

[16] M. Mondal, A. Kamlapure, M. Chand, G. Saraswat, S. Kumar, J. Jesudasan, L. Benfatto, V. Tripathi, and P. Raychaudhuri, Phys. Rev. Lett. **106**, 047001 (2011).

[17] M. Gabay and A. Kapitulnik, Phys. Rev. Lett. **71**, 2138 (1993).

[18] L. Benfatto, C. Castellani, and T. Giamarchi, Phys. Rev. Lett. **98**, 117008 (2007).

[19] L. Benfatto, C. Castellani, and T. Giamarchi, Phys. Rev. B **77**, 100506(R) (2008).

[20] S. Raghu, D. Podolsky, A. Vishwanath, and David A. Huse, Phys. Rev. B **78**, 184520 (2008).

[21] L. Benfatto, C. Castellani, and T. Giamarchi, Phys. Rev. B **80**, 214506 (2009).

[22] S. P. Chockalingam, Madhavi Chand, John Jesudasan, Vikram Tripathi, and Pratap Raychaudhuri, Phys. Rev. B **77**, 214503 (2008); J. Phys. Conf. Ser. **150**, 052035 (2009).

[23] D. J. Bishop and J. D. Reppy, Phys. Rev. B **22**, 5171 (1980).

[24] To account for the finite length scale [13,19] $r_\omega = \sqrt{14D/\omega} \sim 0.1$ mm ($D \sim \hbar/m$ being the diffusion constant of vortices) set in by the ac probing field, we used a finite cutoff $\ell_{\max} = \ln(r_\omega/\xi_0) \sim 10$ ($\xi_0 \sim 5$ nm) in the numerical integration of our RG equations [19]. A similar cutoff is obtained by considering the Pearl length [13] $\Lambda = 2\lambda^2/d$ due to the screening of supercurrents. Indeed, for our sample, we obtain $\Lambda \sim 1$ mm close to T_{BKT}. In both cases, such a cutoff has a negligible smearing effect, which is anyway screened by the broadening resulting from inhomogeneities in the sample [19,21].

[25] N. Nagaosa, *Quantum Field Theory in Condensed Matter* (Springer, New York, 1999).

[26] S. Kirkpatrick, Rev. Mod. Phys. **45**, 574 (1973).

[27] S. Caprara, M. Grilli, L. Benfatto, and C. Castellani, Phys. Rev. B **84**, 014514 (2011).

[28] G. M. Bruun and L. Viverit, Phys. Rev. A **64**, 063606 (2001).

[29] P. G. de Gennes, *Superconductivity in Metals and Alloys* (Benjamin, New York, 1966).

[30] G. Seibold, L. Benfatto, C. Castellani, and J. Lorenzana, arXiv:1107.3839.

[31] G. Seibold *et al.* (to be published).

[32] A. Ghosal, M. Randeria, and N. Trivedi, Phys. Rev. B **65**, 014501 (2001); K. Bouadim, Y. L. Loh, M. Randeria, and N. Trivedi, Nature Phys. **7**, 884 (2011).

[33] The numerical analysis of weaker couplings would require a substantial increase of the system size. We already take N much larger ($N = 600$ sites) than analogous studies [30,32] of disordered superconductors.